Journal of The Electrochemical Society, 2021 **168** 120548
1945-7111/2021/168(12)/120548/8/$40.00 © 2021 The Electrochemical Society ("ECS"). Published on behalf of ECS by IOP Publishing Limited

Reducing the Self-Discharge Rate of Supercapacitors by Suppressing Electron Transfer in the Electric Double Layer

Mingwei Shi,[1,2] Zailei Zhang,[1,2] Man Zhao,[1,2] Xianmao Lu,[1,2,z] and Zhong Lin Wang[1,2,3,z]

[1]*CAS Center for Excellence in Nanoscience, Beijing Institute of Nanoenergy and Nanosystems, Chinese Academy of Sciences, Beijing 100083, People's Republic of China*
[2]*School of Nanoscience and Technology, University of Chinese Academy of Sciences, Beijing 100049, People's Republic of China*
[3]*School of Materials Science and Engineering, Georgia Institute of Technology, Atlanta, GA 30332–0245, United States of America*

For supercapacitors, high self-discharge rate is an inevitable issue that causes fast decay of cell voltage and loss of stored energy. Designing supercapacitors with suppressed self-discharge for long-term energy storage has been a challenge. In this work, we demonstrate that substantially reduced self-discharge rate can be achieved by using highly concentrated electrolytes. Specifically, when supercapacitors with 14 M LiCl electrolyte are charged to 0.80 V, the open circuit voltage (OCV) drops to 0.65 V in 24 h. In stark contrast, when the electrolyte concentration is reduced to 1 M, the OCV drops from 0.80 to 0.65 V within only 0.3 h, which was 80 times faster than that with 14 M LiCl. Decreased OCV decay rate at high electrolyte concentration is also confirmed for supercapacitors with different electrolytes (e.g., $LiNO_3$) or at higher charging voltages (1.60 V). The slow self-discharge in highly concentrated electrolyte can be largely attributed to impeded electron transfer between the electrodes and electrolyte due to the formation of hydration clusters and reduced amount of free water molecules, thereby faradaic reactions that cause fast self-discharge are reduced. Our study not only supports the newly revised model about the formation of electric double layer with the inclusion of electron transfer, but also points a direction for substantially reducing the self-discharge rate of supercapacitors.
© 2021 The Electrochemical Society ("ECS"). Published on behalf of ECS by IOP Publishing Limited. [DOI: 10.1149/1945-7111/ac44b9]

Manuscript submitted November 2, 2021; revised manuscript received December 9, 2021. Published December 30, 2021.

Supplementary material for this article is available online

Supercapacitors (SCs) based on the electric double layer mechanism have attracted considerable interest in recent years due to their high power density, excellent low-temperature performance, as well as long cycling life.[1] On the other hand, current SCs are facing two main challenges: low energy density and high self-discharge rate. While the former issue has drawn significant attention of researchers in discovering new electrode materials and electrolytes to gain improved energy density,[2] the latter has seriously limited the applications of SCs in long-term energy storage and deserves more in-depth studies.[3–8]

A few strategies have been attempted to date to suppress the self-discharge of SCs based on proposed mechanisms including charge redistribution, faradaic reaction, and ohmic leakage.[6,9–16] For instance, Black et al. examined the effect of charge redistribution on the self-discharge of SCs and found that reduced charge redistribution can be achieved by increasing the charging duration and decreasing the charging current,[17] although this approach requires additional energy and longer charging time. Nematic liquid crystal (5CB, 4-n-pentyl–4′-cyanobiphenyl)[15,18] or nematic hybrid liquid crystal[19] have been introduced as additives to electrolytes to suppress the self-discharge of SCs via electrorheological effect. In addition, self-discharge of SCs may also be suppressed by modifying separators with ionic polyelectrolytes,[2] employing piezoelectric separators,[20] or using solid electrolytes such as poly(ethylene oxide) incorporated with bentonite clay and ionic liquid.[12]

Recently, super-concentrated salt solutions (or "water-in-salt" electrolytes) have been employed as electrolytes for SCs with expanded electrochemical stability window. This type of electrolytes presents evident advantages compared to organic electrolytes because of their high ionic conductivity, improved safety and environmental friendliness, and low cost.[21,22] However, the effect of using highly concentrated electrolytes on the self-discharge of SCs has not been fully understood and further detailed investigation is necessary. In this work, we employed highly concentrated aqueous solutions as electrolytes for activated carbon (AC)-based SCs and examined their self-discharge processes systematically. It was found that the decay of open circuit voltage (OCV) of the SCs drastically decreased with the increase of electrolyte concentration. Specifically, when SC cells with 1 M LiCl electrolyte were charged to 0.80 V, the OCV dropped to 0.65 V in 0.3 h; while for cells with 14 M LiCl electrolyte, the same OCV drop from 0.80 to 0.65 V took 24 h, a duration that was extended for 80 times. Similar trends were obtained for SCs charged to a high voltage of 1.6 V as well as cells using $LiNO_3$ electrolyte. Mechanistic analyses indicate that as the concentration of LiCl increases, the amount of free water molecules in the electrolyte solution decreases due to the formation of $(Li^+(H_2O)_2Cl^-)_n$ hydration clusters.[23,24] Based on the newly revised model about the formation of the electric double layer with including electron transfer at liquid-solid interface, the electron transfer due to the electron cloud overlap between free water molecules in the electrolyte and solid atoms of the electrodes may be reduced with the increase of electrolyte concentration.[25,26] This impeded electron transfer in highly concentrated electrolyte can lead to slower faradaic reactions and hence much reduced self-discharge of the SCs. The results of this work demonstrate that using highly concentrated electrolytes can be a simple and effective strategy to achieve much suppressed self-discharge for supercapacitors.

Experimental Section

Chemicals and materials.—Activated carbon (AC) powder (YEC-8A) was purchased from Yihuan Carbon Co. Ltd (Fuzhou, China). Lithium chloride (LiCl, 99%) and lithium nitrate ($LiNO_3$, 99.9%) were purchased from Aladdin Reagent Co. Ltd (Shanghai, China). All chemicals and solvents were employed as received without any further purification. All aqueous solutions were prepared with ultrapure deionized water.

Preparation of electrodes and AC ink.—For the preparation of electrodes, AC, acetylene black, and polyvinylidene difluoride (PVDF) binder were mixed in a mass ratio of 80:10:10 and dispersed in n-methyl-2-pyrrolidone (NMP) to form a uniform slurry. The slurry was coated onto titanium (Ti) substrates (1×1 cm^2 each) for LiCl electrolyte or stainless steel (SS) substrates (1×1 cm^2 each) for $LiNO_3$ electrolyte. Titanium (Ti) substrates were selected as the current collectors for LiCl electrolyte to avoid corrosion by Cl^- ions.

[z]E-mail: luxianmao@binn.cas.cn; zhong.wang@mse.gatech.edu

The resulting electrodes were dried under vacuum at 120 °C overnight. The mass loading of AC on each electrode was 1 mg cm^{-2}.

AC ink was prepared by adding 10 mg of AC to a mixture of ethanol (1 ml) and Nafion solution (20 μl).Then the mixture was treat with ultra-sonication for 30 min. After that, the ink (10 μl) was deposited on a 5 mm diameter glassy carbon disk and evaporated the solvent in air at room temperature.

Characterizations.—The electrochemical experiments were carried out in a symmetric two-electrode system with an additional saturated calomel electrode (SCE) as the reference to monitor the potential of each electrode. Cyclic voltammetry (CV) and galvanostatic charge-discharge (GCD) measurements were conducted on a Solartron 1287 A potentiostat. Electrochemical impedance spectroscopy (EIS) measurements were conducted on a Solartron 1260 A impedance analyzer over a frequency range from 10^6 to 0.1 Hz at an AC amplitude of 10.0 mV. Cycling stability tests were acquired by a LAND CT2001A battery test system. The self-discharge experiments were performed using an Arbin BT2000 battery testing system.

Before self-discharge measurements, the symmetric two-electrode cells were cycled for 50 times by CV from 0 V to the desired voltages (0.80 V or 1.60 V) at a scan rate of 50 mV s^{-1}, then the cells were charged and discharged at 0.2 A g^{-1} between 0 V and the desired voltages (0.80 V or 1.60 V) for 20 cycles. For self-discharge experiments, the cells were charged at 0.2 A g^{-1} from the open circuit cell potential to the desired voltages (0.80 or 1.60 V) which were further held for 2 h (float voltage), during which the current responses (so-called leakage currents) were recorded. After 2 h of potentiostatic period at the specified voltage, the applied voltage was removed and the OCPs of the electrodes were recorded.

Linear sweep voltammetry (LSV) tests were performed using a three-electrodes cell, in which a platinum plate was used as the counter electrode, saturated calomel electrode (SCE) electrode as the reference electrode, and activated carbon on a rotating disk electrode (Princeton Applied Research) as the working electrode. LSV results were recorded using a CHI660E electrochemical workstation at room temperature.

Results and Discussion

Electrochemical performances.—SCs were assembled with LiCl electrolytes of different concentrations ranging from 1 to 14 M. Electrochemical tests showed that, for all electrolyte concentrations, pseudo-rectangular cyclic voltammograms (CVs) were obtained below 0.80 V (Fig. 1a). Noticeable deviation from typical rectangular shape was observed when the CVs were scanned to 1.6 V for low-concentration electrolytes, but only slightly for 14 M LiCl (Fig. 1b), suggesting wider voltage window for higher electrolyte concentration. This was also confirmed from galvanic charge/discharge (GCD) curves, which revealed nearly symmetric triangular shape when the SCs with 1 and 14 M LiCl electrolytes were charged to voltages up to 1.00 and 1.60 V, respectively. Based on the charge/discharge curves, the capacitances of the SCs were estimated to be 90 F g^{-1}. Figure 1e shows that the Nyquist plot of each SC consisted of an incomplete semicircle at the high frequency region and a straight line at the low frequency region, with an equivalent series resistance (ESR) in the range of 3–7 ohms. The cycling stability of the SCs was also evaluated (Fig. 1f). For SCs with 14 M LiCl, the capacitance retentions at 2 A g^{-1} after 10000 cycles were 99% and 92% when charged to 0.80 and 1.60 V, respectively. It is worth noting that with the progress of cycling test, capacitances higher than the initial value were observed for some cycles. This may be due to incomplete infiltration of the electrolyte into the pores of the electrode in the beginning.

Evaluation of self-discharge rates.—The self-discharge rates of the SCs were evaluated based on OCV decay and leakage current. It was found that the self-discharge rate of the SCs dropped substantially with the increase of electrolyte concentration. Figure 2a shows the OCV decays after the cells were charged to 0.80 V and maintained at the voltage for 2 h. Upon removal of the applied voltage, the OCVs of the SCs dropped from 0.80 V to 0.12, 0.18, 0.30, 0.48, and 0.65 V after 24 h for 1, 5, 9, 10, and 14 M LiCl electrolytes, respectively. Clearly, the OCV of the cell with 14 M electrolyte dropped much slower than that with 1 M electrolyte. In addition, to reach the same OCV drop of 0.15 V (i.e., from 0.8 to 0.65 V), it took 0.3, 1.9, 5.0, 6.7, and 24 h for the SCs with 1, 5, 9, 10 and 14 M LiCl electrolytes, respectively (Fig. 2b). This result indicates that the duration to maintain cell voltage above 0.65 V was extended for more than 80 times when the electrolyte concentration increased from 1 to 14 M. Similarly, for SCs charged to 1.60 V, the OCVs dropped respectively to 0.11, 0.43, 0.69, 0.86 and 1.23 V after 24 h for 1, 5, 9, 10, and 14 M LiCl electrolytes (Fig. 2c). The duration to reach the same OCV drop of 0.37 V (i.e., from 1.60 to 1.23 V) was 40 times longer for 14 M electrolyte than that of 1 M electrolyte (Fig. 2d). Based on the above results, it is evident that the SCs with highly concentrated 14 M LiCl electrolyte exhibited drastically reduced self-discharge rate than lower electrolyte concentrations.

Leakage current measured with an applied float voltage is another important parameter to evaluate the self-discharge of SCs.[27–30] As shown in Figs. 2e–2h, the leakage currents for the SCs decreased substantially with the increase of electrolyte concentration. For 1 M LiCl, the leakage current at 0.80 V was 8 μA after 2 h, but it was reduced to 0.3 μA for 14 M LiCl electrolyte (27 times smaller than 1 M LiCl electrolyte). Similarly, with a float voltage of 1.60 V, the leakage current for 1 M LiCl electrolyte stabilized at 21 μA after 2 h, while for 14 M LiCl, the leakage current dropped to 2 μA. This result further confirms that the self-discharge of the SCs was largely suppressed at high LiCl concentration.

Mechanistic analysis.—For SCs based on electric double layer mechanism, three self-discharge pathways have been proposed: (1) internal ohmic leakage; (2) faradaic reactions with either activation- or diffusion-controlled mechanism; (3) charge redistribution near the electrode surface.[5,16,30–36] Of the three, ohmic leakage is the most straightforward mechanism which simply arises from leakage currents passing through resistive pathways between the positive and negative electrodes.[5,10,12,13] For self-discharge caused by faradaic reactions, it is attributed to oxidation or reduction reactions occurring at the electrode/electrolyte interface. In this case, the self-discharge rate is dependent on the rate limiting step of the faradaic reaction: if the reaction rate is limited by the electron transfer across the double-layer, the self-discharge can be attributed to activation-controlled mechanism; if the diffusion of the reacting species/ions toward the electrode is the rate limiting step, it is called diffusion-controlled mechanism.[5,10,12,13] Lastly, self-discharge caused by charge redistribution mainly occurs on the surface of porous electrodes where the movement of surface charges leads to decreased cell voltage.[5,10,12,13] Examining the change in open circuit potential (OCP) of both positive and negative electrodes of a SC may afford further insight into the self-discharge mechanisms, especially with considering the newly revised model about the formation of the electric double layer by including electron transfer at liquid-solid interface.[25,26]

For ohmic leakage, the change of electrode OCP (V_t) with discharge time t is given as:[5,14,15,34,37]

$$V_t = V_i \exp\left(-\frac{t}{RC}\right) \quad [1]$$

where V_i is the initial electrode potential of the charged SC, C is the capacitance, R is universal gas constant, and RC corresponds to the time constant of the self-discharge process.

For activation-controlled faradaic process, the change of V_t *vs* ln (t) would give a straight line[5,14,15,34].

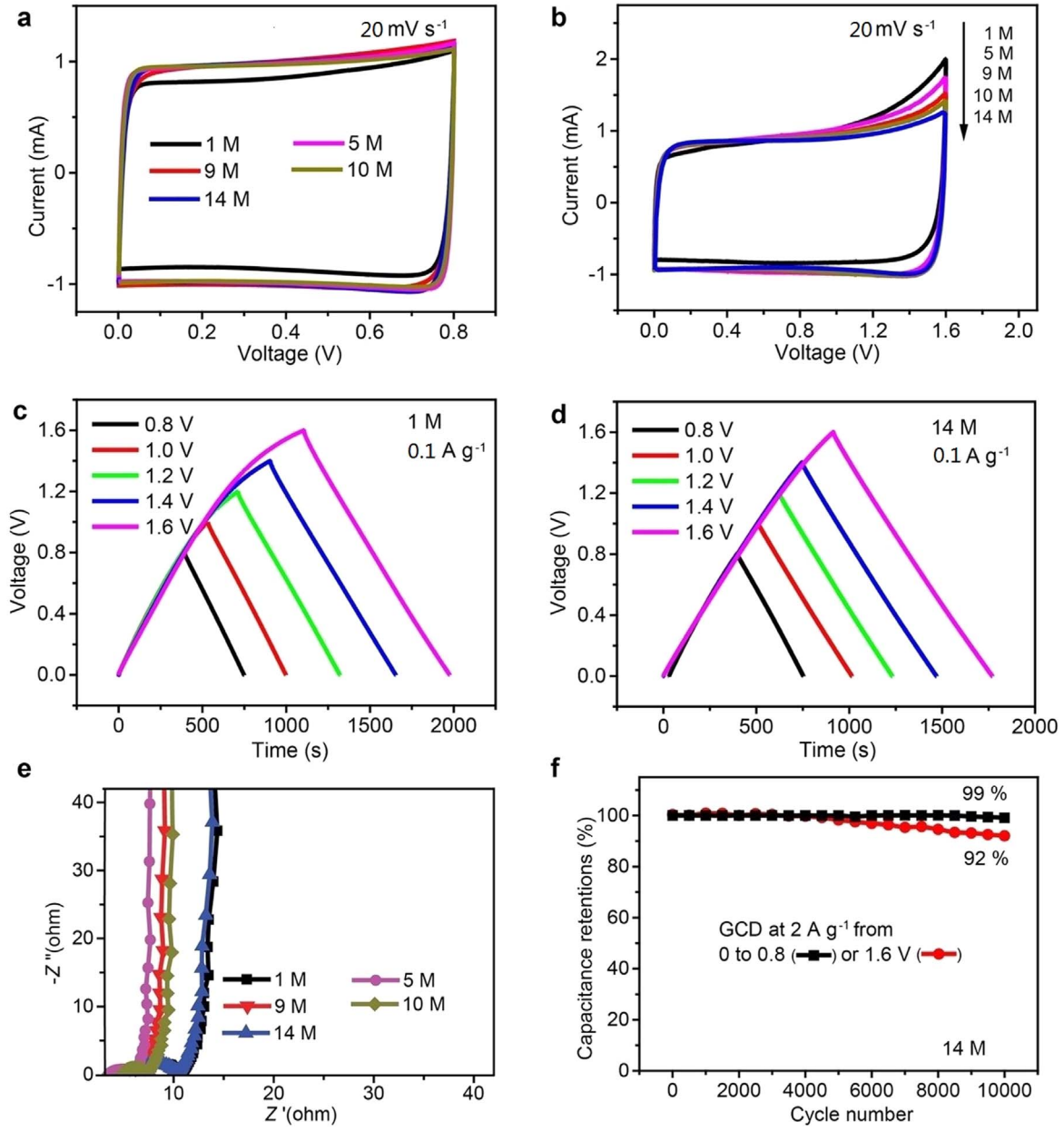

Figure 1. Electrochemical performances of SCs with LiCl electrolyte. (a), (b) CV curves of SCs using 1, 5, 9, 10, and 14 M LiCl electrolytes with a cell voltage of (a) 0.80 V and (b) 1.60 V at a scan rate of 20 mV s^{-1}. (c), (d) GCD curves of SCs using (c) 1 M and (d) 14 M LiCl electrolytes with cell voltages of 0.80–1.60 V. (e) EIS of SCs with 1, 5, 9, 10, and 14 M LiCl electrolytes. (f) Cycling stability of SCs using 14 M LiCl electrolyte with cell voltages of 0.80 and 1.60 V.

$$V_t = -\frac{RT}{\alpha F} ln \frac{\alpha F i_0}{RTC} - \frac{RT}{\alpha F} \ln\left(t + \frac{CK}{i_0}\right) \quad [2]$$

which can be simplified as

$$V_t = V_i - a - bln\left(t + \frac{CK}{i_0}\right) \quad [3]$$

where T is the absolute temperature, α is the charge transfer coefficient, F is Faraday constant, i_0 is the exchange current density, K is an integration constant, and a, b are constants related to the faradaic process.

For diffusion-controlled faradaic process, the potential would decline with the $t^{1/2}$:[38–40]

$$V_t = V_i - \frac{2zFSD^{1/2}\pi^{1/2}c_0}{C} t^{1/2} \quad [4]$$

which can be re-written as

$$V_t = V_i - mt^{1/2} \quad [5]$$

where D is the diffusion coefficient of the redox species, z is the charge, c_0 is the initial concentration, S is the electroactive surface area, and m is a constant related to the diffusion coefficient of the redox species.

Combining the potential decays caused by above three mechanisms, the following general formula can be used to fit the self-discharge curve $V_t = f(t)$:[15]

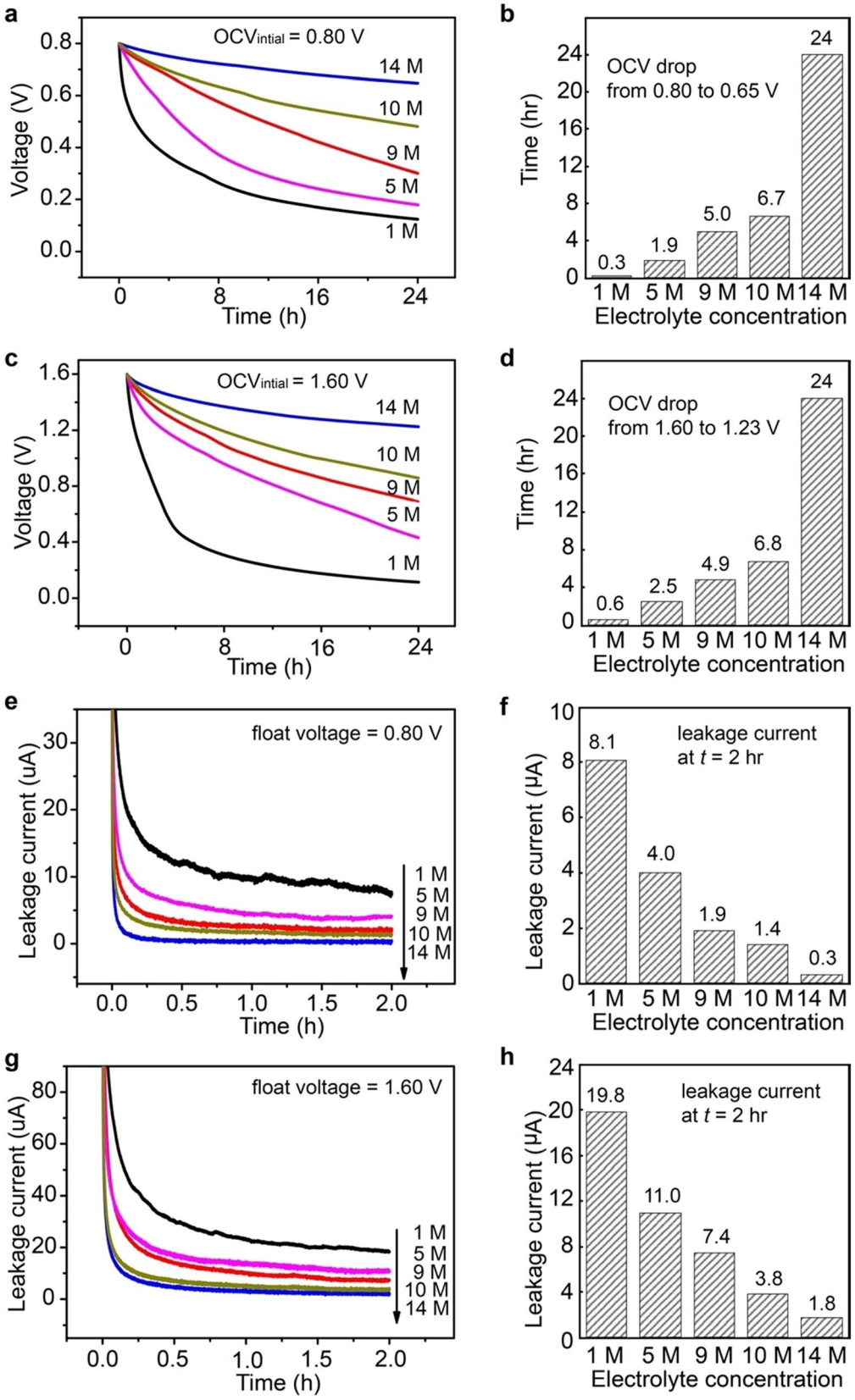

Figure 2. Self-discharge of SCs with LiCl electrolyte of various concentrations. (a) OCV decay profiles for SCs charged to 0.80 V and (b) the times taken for OCV to drop from 0.80 to 0.65 V. (c) OCV decay profiles for SCs charged to 1.60 V and (d) the times taken for OCV to drop from 1.60 to 1.23 V. (e) Leakage current profiles for SCs charged to 0.80 V and (f) the currents after 2 h. (g) Leakage current profiles for SCs charged to 1.60 V and (h) the currents after 2 h.

$$V_t = V_i \exp\left(-\frac{t}{RC}\right) - mt^{1/2} - a - bln\left(t + \frac{CK}{i_0}\right) \quad [6]$$

With a saturated calomel electrode (SCE) as the reference, we monitored the OCP decays of both positive and negative electrodes in the cells. As shown in Figs. 3a–3b, when the SCs were charged to 0.80 V, the potentials of the positive electrodes for 1, 5, 9, 10, 14 M electrolytes dropped from 0.86 to 0.58 V, from 0.78 to 0.60 V, from 0.78 to 0.62 V, from 0.76 to 0.66 V, and from 0.76 to 0.68 V (vs SHE) after 12 h, respectively. In the meantime, the potentials of the corresponding negative electrodes increased from 0.02 to 0.37 V, from −0.02 to 0.31 V, from −0.02 to 0.12 V, from −0.04 to 0.06 V, and from −0.04 to −0.01 V (vs SHE) for 1, 5, 9, 10, 14 M electrolytes, respectively. Both positive and negative electrodes contributed to the self-discharge of the SCs. With the increase of the electrolyte concentration, the potential changes of both positive and negative electrodes decreased, again confirming suppressed self-discharge at higher electrolyte concentration.

The OCP profiles of the positive and negative electrodes were then fitted by the self-discharge mechanisms based on Eqs. 1–6 with parameters listed in table S1–S4 (available online at stacks.iop.org/JES/168/120548/mmedia), Supplemental Information. It is clear that different self-discharge pathways contributed differently with the change in electrolyte concentration. For 1 and 5 M LiCl electrolytes, the potential changes for both positive and negative electrodes fitted well with the activation-controlled faradaic model. For 10 and 14 M LiCl electrolytes, the simulated potential changes matched closely with the diffusion-controlled faradaic model. For 9 M electrolyte, the potential drop of the positive electrode can be attributed to a mixed activation- and diffusion-controlled faradaic process, but the potential increase of the negative electrode matched better with activation-controlled faradaic process.

Similar results were obtained from the SCs charged to a high voltage of 1.60 V (Figs. 3c, 3d)-while at lower electrolyte concentrations of 1 and 5 M, activation-controlled faradaic process dominated the self-discharge of both positive and negative electrodes; at higher concentrations of 10 and 14 M, the self-charge was mainly caused by diffusion-controlled faradaic process; and with 9 M LiCl electrolyte, both activation- and diffusion-controlled faradaic processes of the positive and negative electrodes played a part in the overall OCV decay of the cell.

The above simulation results suggest that, with the increase of the electrolyte concentration, a transition from activation-controlled to diffusion-controlled faradaic self-discharge process occurred. This transition may be explained with the decrease of the amount of free water molecules in the LiCl electrolyte at higher concentrations. Activated carbon (AC)-based electrodes possess high specific surface area and oxygen-based surface functionalities (mainly quinone, carbonyl, phenol, lactone and anhydride groups).[41] With an aqueous electrolyte, side reactions may take place on the AC electrodes such as oxidation and reduction of carbon surface groups, O_2 evolution, carbon corrosion, and generation of hydrogen. Detailed analysis of the effect of these reactions on the stability of the electrodes in high-voltage SCs has been reported before.[41] It is expected that these side reactions not only can affect the electrochemical performance of SCs, such as specific capacitance, internal resistance, and cycle stability,[41–46] but also contribute significantly on the self-discharge process.[4,29,47–49] On positive electrodes, oxygen-based surface functionalities of AC can be oxidized to form CO and CO_2[26,41,47,50] and water can be decomposed to releases oxygen.[27,41,46] On the negative electrode, surface functional groups containing sp-hybridized oxygen such as quinone and carbonyl groups can be reduced and electro-reduction of water may occur.[41–45]

When a SC is fully charged, the above side reactions may consume the stored charges on the electrodes, causing self-discharge

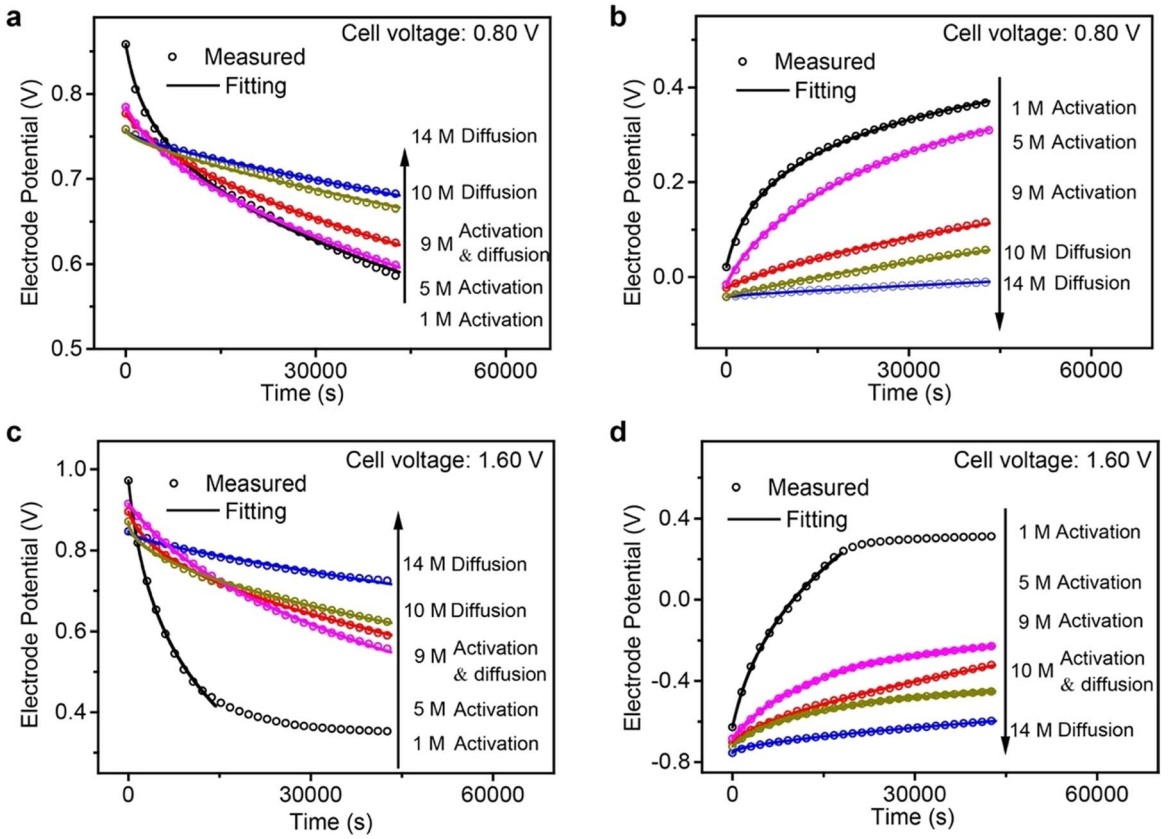

Figure 3. OCP profiles and the corresponding fitting curves of SC electrodes with LiCl electrolyte of various concentrations. (a) Positive and (b) negative electrodes for cells charged to 0.80 V. (c) Positive and (d) negative electrodes for cells charged to 1.60 V.

of the SC. Notably, most of these side reactions require the participation of water,[41] and the rate of these side reactions can be largely affected by both the availability of free water molecules near the electrode surface as well as the rate of electron transfer. Therefore, one can expect that with highly concentrated LiCl electrolyte, water molecules are largely bound to the ions to form hydration clusters $[Li^+(H_2O)_nCl^-]$, leaving reduced amount of free water molecules.[23] Moreover, due to decreased amount of free water molecules, the rates of these faradaic reactions are more determined by the diffusion of free water molecules, leading to the shift of the self-discharge process from activation-controlled to diffusion-controlled faradaic mechanism. It is noted that the average binding energy between one water molecule and Li^+ ion is about 1.0 eV, and the average water-water binding energy is about 0.27 eV per molecule.[51] As the interaction between water molecule and Li^+ ion is much stronger than the hydrogen bond between water molecules, it is more difficult for water molecules to overcome the energy barrier and escape from hydration clusters to participate in the side reactions at high LiCl concentrations.

The increased electrolyte concentration may also impede the charge transfer caused by electron exchange between redox molecules and electrode surface due to the overlap of the electron clouds of the solid atoms and the reactive molecules.[52] Recent studies by Wang et al. have revealed that both ion transfer and electron transfer take place at the liquid-solid interface within the electric double layer formed when an electrode is in contact with electrolyte.[25,26] They found that electron transfer occurs first before ion transfer. The high mobility and thermal instability of electrons at interface can contribute to the instability of the electric double layer, resulting in a large discharging rate. For electrochemical reactions at the electrode, the solvent and supporting electrolyte concentration can affect the electron transfer kinetics and the reaction rate significantly. Also, the change of dielectric environment around the reactive species due to the increased electrolyte concentration and hence smaller dielectric constant also impedes electron transfer that is required for faradaic processes.[53,54]

Evaluation of oxygen reduction reaction rates.—To examine the change in electron transfer kinetics with electrolyte concentration, we measured the oxygen reduction reaction (ORR) rates of activated carbon in LiCl electrolytes saturated with O_2. ORR test was chosen because side reactions involving oxygen can contribute largely to the self-discharge of supercapacitors. As shown in Fig. 4, the ORR kinetics was significantly affected by the electrolyte concentration. Both the onset and half-wave potentials shifted negatively with the increase of LiCl concentration. Especially for 14 M LiCl, the ORR half-wave potential was nearly 110 mV more negative than that of 1 M LiCl (0.07 V vs SHE for 1 M LiCl and −0.04 V vs SHE for 14 M LiCl). The much negatively shifted half-wave potential and therefore sluggish kinetics of ORR in 14 M LiCl suggest much reduced electron transfer rate in electrolyte of higher concentration, which led to much slower self-discharge.

Effect of different electrolyte ions and float charging on self-discharge.—The effect of electrolyte concentration on the self-discharge of SCs was further confirmed using $LiNO_3$ electrolyte. For SCs charged to 0.80 V, the OCVs dropped to 0.12 and 0.65 V after 24 h for 1 and 14 M $LiNO_3$ electrolytes (Fig. 5a). Similarly, for SCs charged to 1.60 V, the OCVs dropped to 0.11 and 1.12 V after 24 h for 1 and 14 M $LiNO_3$ electrolytes (Fig. 5b). The large difference in OCV drop rate clearly indicates that the electrolyte concentration has an immense effect on the self-discharge of SCs.

When SCs are used for fast charging/discharging applications, maintaining a float voltage for a long time may not be an available option, even though this strategy has been widely reported for self-discharge mitigation. In this case, examining the self-discharge rate without float charging would be more meaningful for practical applications. Therefore, we measured the OCV decays of SCs with 14 M LiCl electrolyte after the cells were charged at 0.2 A g^{-1} to 0.80 or 1.60 V without float charging (Figs. 5c–5d). It is clearly revealed that the self-discharge rate of 14 M LiCl electrolyte was much reduced compared to that of 1 M LiCl without applying a float voltage. For SCs with 1 and 14 M LiCl electrolytes charged to 0.80 V, the OCV dropped to 0.06 and 0.44 V after 24 h, respectively. While for SCs charged to 1.60 V, the OCV dropped to 0.08 and 1.00 V after 24 h for 1 and 14 M LiCl, respectively. The SCs with 14 M LiCl electrolyte exhibited much suppressed self-discharge rate even without float charging, suggesting that such SCs could be combined with environmental energy harvesting devices for fast charging/discharging and improved energy storage efficiencies.

Conclusions

In summary, we have demonstrated that simply increasing electrolyte concentration can effectively reduce the self-discharge rate of SCs. Notably, SCs with 14 M LiCl electrolyte exhibited a high operating voltage (1.60 V), low leakage current (10 times smaller than that of 1 M LiCl electrolyte), and slow OCV decay (24 h from 1.60 to 1.23 V, which was 40 times longer than that of 1 M LiCl electrolyte). The slower self-discharge at higher concentrations of electrolyte can be attributed to the increased number of hydration clusters and decreased amount of free water molecules that lead to reduced rate of electron transfer and faradaic side reactions. The results of this study support the newly revised model about the formation of electric double layer with the inclusion of electron transfer. It also suggests that increasing electrolyte concentration can be a simple and effective strategy for designing SCs with much

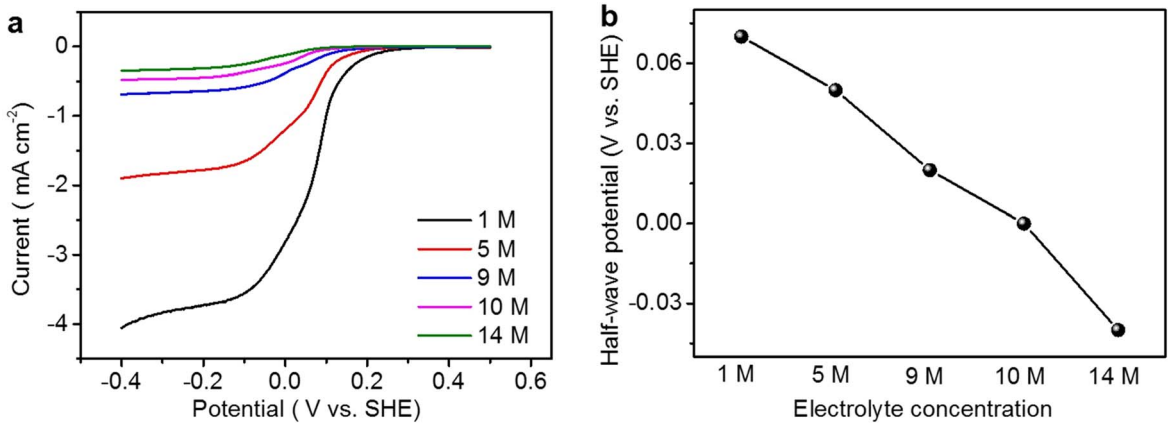

Figure 4. Oxygen reduction reaction (ORR) in O_2-saturated LiCl electrolyte of various concentrations. (a) Linear sweep voltammetry (LSV) of activated carbon on a rotating disk electrode (RDE) at a revolution of 1600 rpm and a scan rate of 10 mV s^{-1}. (b) Decreasing ORR half-wave potential with electrolyte concentration.

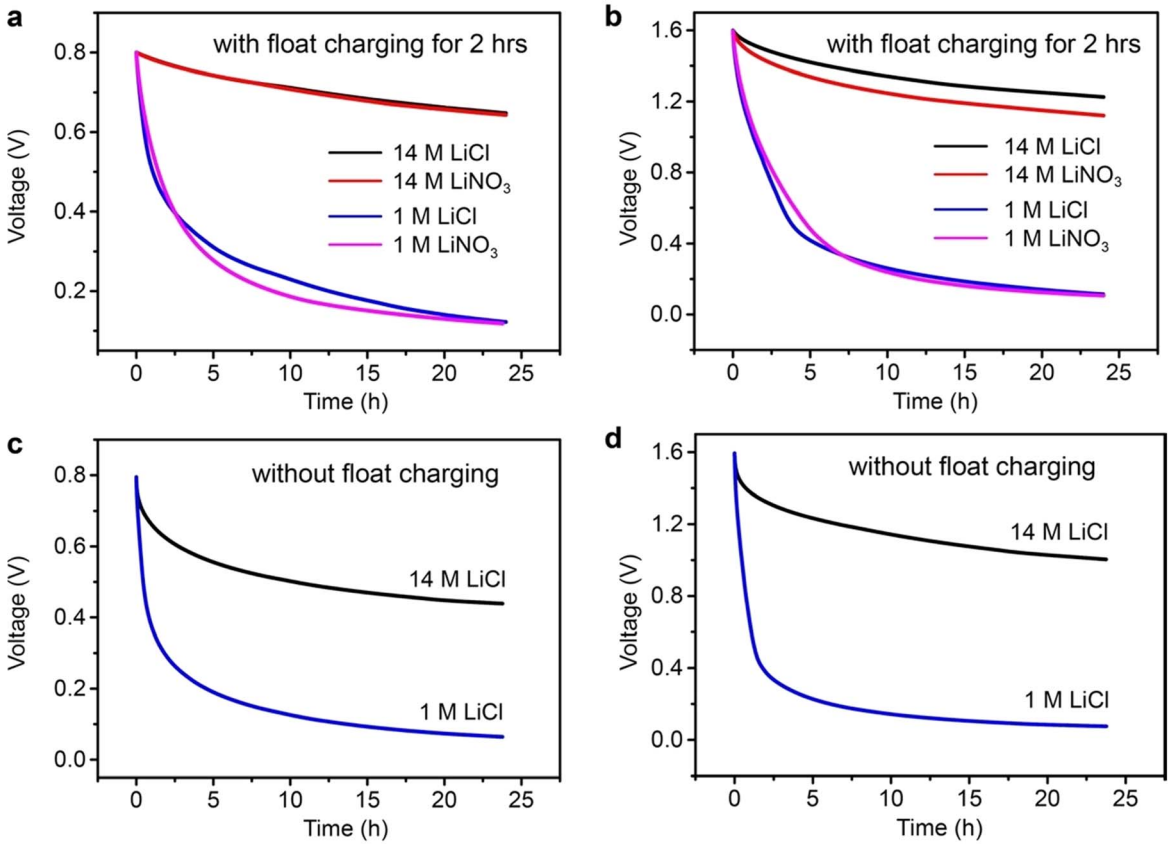

Figure 5. Self-discharge profiles for SCs with LiCl and $LiNO_3$ electrolytes. (a), (b) OCV decays of SCs with 1 and 14 M $LiNO_3$ electrolytes charged to (a) 0.80 V and (b) 1.60 V with float charging for 2 h. (c), (d) OCV decays of SCs with 1 and 14 M LiCl electrolytes charged to (c) 0.80 V and (d) 1.60 V without float charging.

suppressed self-discharge. Such SCs may offer both prolonged energy storage and improved charging efficiency from environmental energy harvesting devices.

Acknowledgments

This work was supported by the National Key R & D Project from Minister of Science and Technology (2016YFA0202702) and the National Natural Science Foundation of China (Fund# 21905026).

ORCID

Xianmao Lu https://orcid.org/0000-0002-7422-2867

References

1. Z. Chen, W. Li, J. Yang, J. Liao, C. Chen, Y. Song, S. A. A. Shah, Z. Xu, and M. Wu, *J. Electrochem. Soc.*, **167**, 050506 (2020).
2. H. Wang, Q. Zhou, B. Yao, H. Ma, M. Zhang, C. Li, and G. Shi, *Adv. Mater. Interfaces*, **5**, 1701547 (2018).
3. S. A. Kazaryan, G. G. Kharisov, S. V. Litvinenko, and V. I. Kogan, *J. Electrochem. Soc.*, **154**, A751 (2007).
4. S. A. Kazaryan, S. V. Litvinenko, and G. G. Kharisov, *J. Electrochem. Soc.*, **155**, A464 (2008).
5. H. A. Andreas, *J. Electrochem. Soc.*, **162**, A5047 (2015).
6. L. Chen, H. Bai, Z. Huang, and L. Li, *Energy Environ. Sci.*, **7**, 1750 (2014).
7. A. Lewandowski, P. Jakobczyk, M. Galinski, and M. Biegun, *Phys. Chem. Chem. Phys.*, **15**, 8692 (2013).
8. J. Kowal, E. Avaroglu, F. Chamekh, A. Šenfelds, T. Thien, D. Wijaya, and J. Power, *Sources*, **196**, 573 (2011).
9. Y. Z. Wang, X. Shan, D. Wang, H. Cheng, and F. Li, *J. Energy Chem.*, **38**, 214 (2019).
10. Z. Wang et al., *J. Mater. Chem. A*, **7**, 8633 (2019).
11. H. Zhou, Q. Ma, W. Yang, and X. Lu, *ChemNanoMat*, **6**, 280 (2020).
12. H. Zhao, H. Zhang, Z. Wang, X. Jiang, Y. Xie, Z. Xu, Y. Wang, and W. Yang, *ChemSusChem*, **14**, 3895 (2021).
13. Z. Wang, Z Xu, H Huang, X Chu, Y Xie, D Xiong, C Yan, H Zhao, H Zhang, and W Yang, *ACS Nano*, **14**, 4916 (2020).
14. I. S. Ike, I. Sigalas, and S. E. Iyuke, *Phys. Chem. Chem. Phys.*, **18**, 661 (2015).
15. M. Xia, J. Nie, Z. Zhang, X. Lu, and Z. Wang, *Nano Energy*, **47**, 43 (2018).
16. M. Liu, M. Xia, R. Qi, Q. Ma, M. Zhao, Z. Zhang, and X. Lu, *ChemElectroChem*, **6**, 2531 (2019).
17. J. Black and H. A. Andreas, *Electrochim. Acta*, **54**, 3568 (2009).
18. M. Haque, Q. Li, A. D. Smith, V. Kuzmenko, P. Rudquist, P. Lundgren, and P. Enoksson, *J. Power Sources,*, **453**, 227897 (2020).
19. X. Su, W. Jia, H. Ji, and Y. Zhu, *J. Energy Storage*, **41**, 102830 (2021).
20. S. Nohara, H. Wada, N. Furukawa, H. Inoue, and C. Iwakura, *Res. Chem. Intermed.*, **32**, 491 (2006).
21. Z. Tian, W. Deng, X. Wang, C. Liu, C. Li, J. Chen, M. Xue, R. Li, and F. Pan, *Funct. Mater. Lett.*, **10**, 1750081 (2017).
22. D. Xiao, Q. Wu, X. Liu, Q. Dou, L. Liu, B. Yang, and H. Yu, *Chem. Electro. Chem.*, **6**, 439 (2019).
23. L. Petit, R. Vuilleumier, P. Maldivi, and C. Adamo, *J. Chem. Theory Comput.*, **4**, 1040 (2008).
24. L. Suo, O. Borodin, T. Gao, M. Olguin, J. Ho, X. Fan, C. Luo, C. Wang, and K. Xu, *Science*, **350**, 938 (2015).
25. S. Lin, L. Xu, A. C. Wang, and Z. L. Wang, *Nat. Commun.*, **11**, 399 (2020).
26. S. Lin, X. Chen, and Z. L. Wang, *Chem. Rev.* (2021).
27. L. García-Cruz, P. Ratajczak, J. Iniesta, V. Montiel, and F. Béguin, *Electrochim. Acta*, **202**, 66 (2016).
28. X. Sun, Y. An, L. Geng, X. Zhang, K. Wang, Y. Yin, Q. Huo, T. Wei, X. Zhang, and Y. Ma, *J. Electroanal. Chem.*, **850**, 113386 (2019).
29. A. Laheäär, A. Arenillas, and F. Béguin, *J. Power Sources*, **396**, 220 (2018).
30. J. Niu, B. E. Conway, and W. G. Pell, *J. Power Sources*, **135**, 332 (2004).
31. A. D. Jagadale, R. C. Rohit, S. K. Shinde, and D.-Y. Kim, *J. Electrochem. Soc.*, **168**, 090562 (2021).
32. H. A. Andreas, J. M. Black, and A. A. Oickle, *Electrochim. Acta*, **140**, 116 (2014).
33. B. E. Conway, W. G. Pell, and T. C. Liu, *J. Power Sources,*, **65**, 53 (1997).
34. H. Yang and Y. Zhang, *J. Power Sources,*, **196**, 8866 (2011).
35. M. Kaus, J. Kowal, and D. U. Sauer, *Electrochim. Acta*, **55**, 7516 (2010).
36. Y. Diab, P. Venet, H. Gualous, and G. Rojat, *IEEE Trans. Power Electron.*, **24**, 510 (2009).
37. J. Black, H. A. Andreas, and J. Power, *Sources*, **195**, 929 (2010).
38. Q. Zhang, C. Cai, J. Qin, and B. Wei, *Nano Energy*, **4**, 14 (2014).
39. Q. Zhang, J. Rong, D. Ma, and B. Wei, *Energy Environ. Sci.*, **4**, 2152 (2011).
40. Q. Zhang, J. Rong, and B. Wei, *RSC Adv.*, **1**, 989 (2011).

41. M. He, K. Fic, E. Frackowiak, P. Novák, and E. J. Berg, *Energy Environ. Sci.*, **9**, 623 (2016).
42. K. Jurewicz, E. Frackowiak, and F. Béguin, *Appl. Phy. A*, **78**, 981 (2004).
43. P. Ratajczak, K. Jurewicz, and F. BÚguin, *J. Appl. Electrochem.*, **44**, 475 (2014).
44. Q. Gao, L. Demarconnay, E. Raymundo-Piñero, and F. Béguin, *Energy Environ. Sci.*, **5**, 9611 (2012).
45. F. Béguin, K. Kierzek, M. Friebe, A. Jankowska, J. Machnikowski, K. Jurewicz, and E. Frackowiak, *Electrochim. Acta*, **51**, 2161 (2006).
46. B. Avasarala, R. Moore, and P. Haldar, *Electrochim. Acta*, **55**, 4765 (2010).
47. A. M. Oickle, J. Tom, and H. A. Andreas, *Carbon*, **110**, 232 (2016).
48. M. A. Davis and H. A. Andreas, *Carbon*, **139**, 299 (2018).
49. A. M. Oickle and H. A. Andreas, *J. Phys. Chem. C*, **115**, 4283 (2011).
50. Y. B. Xie, Y. Xie, W. Qiao, W. Zhang, G. Sun, and L. Ling, *New Carbon Mater.*, **25**, 248 (2010).
51. J. Zheng et al., *Chem.*, **4**, 2872 (2018).
52. C. Xu et al., *Adv. Mater.*, **30**, 1706790 (2018).
53. G. Das, S. Hlushak, M. C. Ramos, and C. McCabe, *AIChE J.*, **61**, 3053 (2015).
54. A. P. Abbott and J. F. Rusling, *J. Phys. Chem.*, **94**, 8910 (1990).